

J80-043 Flow Patterns Near a Conical Sonic Line

20017
20018

Manuel D. Salas*

NASA Langley Research Center, Hampton, Va.

A study is made in the physical plane of the flow properties near a conical crossflow sonic line. The shapes of the Mach lines at regular and singular sonic points are presented. Through a study of the jump conditions at a singular sonic point, the possibility of a double sonic line is discussed. The properties of bubbles of supersonic crossflow are examined. Numerical results are presented to support some of the theoretical observations.

I. Introduction

CONICAL flows are characterized by having constant flow properties along rays emanating from a common vertex. When the assumption of conicity is imposed on the full Euler equations, the number of independent variables is reduced by one, permitting the investigation of essentially three-dimensional phenomena by means of two-dimensional methods. Recently, the study of conical flows has been extended to incompressible fluids^{1,2}; the present study, however, only treats conical inviscid supersonic flows as originally considered by Busemann in Ref. 3.

In the study of conical flows, it is usually convenient to take advantage of the conical self-similarity of the flow by considering the projection of the flowfield onto the surface of a unit sphere centered at the vertex. On this surface, the governing equations generally exhibit mixed-type behavior, with hyperbolic and elliptic regions separated by boundaries where the velocity component tangent to the unit sphere becomes sonic. The purpose of this paper is to investigate the properties of conical flows in the neighborhood of these boundaries.

Investigations of this nature have been conducted for two-dimensional flows,⁴⁻⁷ with solutions to Tricomi's equation providing much of the fundamental properties peculiar to this transonic region. The significance of these studies toward a better understanding of two-dimensional transonic flows is unquestionable, and it is reasonable to expect that similar studies for conical flows, with their tantalizing insight into three-dimensional flows, should prove equally profitable.

As in two-dimensional flows, the investigation may be conducted in either the physical or hodograph plane. The advantage of the hodograph plane is that on it the equations of motion are linear. Such an approach was taken by Reyn,⁸ who studied the properties of conical flows through the differential geometry of the hodograph transformation. In the present work, the study will be conducted in the physical plane, since as eloquently stated by Lighthill,⁴ in the physical plane "...the results obtained, so far as they go, carry more complete conviction and give greater physical comprehension of affairs than corresponding investigations in the elusive hodograph plane."

The presentation proceeds by first developing the information required to define the flow patterns near a

crossflow sonic line and then, in the last two sections, synthesizing this information to create a picture of the possible flow patterns. Thus, in Sec. II, the governing equations are cast in various forms to be used in subsequent sections. In Sec. III, the flow properties along the sonic line are discussed. The shape of the Mach line is then determined in Sec. IV. Singular sonic points are studied in Sec. V. Finally, in Secs. VI and VII, the previously developed information is used to study possible flow patterns.

II. Governing Equations

It is usually convenient to write the governing equations in spherical polar coordinates, where r is the distance from the conical vertex, θ is the polar angle, and ϕ is the azimuthal angle. With the velocity components u , v , and w taken in the positive directions of r , θ , and ϕ , respectively, the equations of motion on the surface of the unit sphere are given by

$$v\rho_\theta + \frac{w}{\sin\theta}\rho_\phi + \rho(v_\theta + \frac{1}{\sin\theta}w_\phi + 2u + v\cotan\theta) = 0 \quad (1a)$$

$$vu_\theta + \frac{w}{\sin\theta}u_\phi - (v^2 + w^2) = 0 \quad (1b)$$

$$vv_\theta + \frac{w}{\sin\theta}v_\phi + \frac{1}{\rho}p_\theta + uv - w^2\cotan\theta = 0 \quad (1c)$$

$$vw_\theta + \frac{w}{\sin\theta}w_\phi + \frac{1}{\rho\sin\theta}p_\phi + uw + vw\cotan\theta = 0 \quad (1d)$$

$$vS_\theta + \frac{w}{\sin\theta}S_\phi = 0 \quad (1e)$$

with suffixes denoting partial derivatives and p , ρ , and S denoting the pressure, density, and entropy, respectively. The entropy is connected to the pressure and density through the relation

$$S = \ln(p/\rho^\gamma) \quad (2)$$

where γ is the adiabatic exponent.

A somewhat more revealing form of the system of Eqs. (1) is obtained by introducing the magnitude q and inclination β of the crossflow velocity component which are defined by

$$q^2 = v^2 + w^2 \quad (3a)$$

$$\tan\beta = v/w \quad (3b)$$

In terms of these variables, the governing equations are:

$$\left(1 - \frac{a^2}{q^2}\right) \frac{1}{\gamma p} p_s + \beta_n + \frac{u}{q} + \sin\beta\cotan\theta = 0 \quad (4)$$

Presented as Paper 79-0341 at the AIAA 17th Aerospace Sciences Meeting, New Orleans, La., Jan. 15-17, 1979; submitted Jan. 29, 1979; revision received Aug. 24, 1979. This paper is declared a work of the U.S. Government and therefore is in the public domain. Reprints of this article may be ordered from AIAA Special Publications, 1290 Avenue of the Americas, New York, N.Y. 10019. Order by Article No. at top of page. Member price \$2.00 each, nonmember, \$3.00 each. Remittance must accompany order.

Index categories: Transonic Flow; Supersonic and Hypersonic Flow.

*Aero-Space Technologist, Supersonic Aerodynamics Branch, High-Speed Aerodynamics Division. Member AIAA.

$$u_s = q \quad (5)$$

$$q_s + (a^2/\gamma qp)p_s + u = 0 \quad (6)$$

$$\beta_s + (a^2/\gamma q^2 p)p_n - \cos\beta \cotan\theta = 0 \quad (7)$$

$$S_s = 0 \quad (8)$$

where a is the speed of sound and s and n are coordinates that are locally tangent and normal to crossflow streamlines, such that

$$\frac{\partial}{\partial s} = \sin\beta \frac{\partial}{\partial \theta} + \frac{\cos\beta}{\sin\theta} \frac{\partial}{\partial \phi} \quad (9a)$$

$$\frac{\partial}{\partial n} = \cos\beta \frac{\partial}{\partial \theta} - \frac{\sin\beta}{\sin\theta} \frac{\partial}{\partial \phi} \quad (9b)$$

In Eq. (4), the pressure can be eliminated by means of Eq. (6), resulting in

$$\frac{1}{q} \left(1 - \frac{q^2}{a^2} \right) q_s + \beta_n + \frac{u}{q} \left(2 - \frac{q^2}{a^2} \right) + \sin\beta \cotan\theta = 0 \quad (10)$$

Clearly, the system of Eqs. (5-8) and Eq. (10) is elliptic in regions of the unit sphere where $q^2 < a^2$ and hyperbolic in regions where $q^2 > a^2$. The locus of points on the unit sphere where $q^2 = a^2$ forms a boundary between these regions will be referred to as the crossflow sonic line.

If the flow is irrotational (see Appendix), Eq. (7) may be replaced by the following equation

$$q_n + (a^2/\gamma qp)p_n = 0 \quad (11)$$

As in two-dimensional supersonic flows, in hyperbolic regions on the surface of the unit sphere, we may define at each point two real characteristic directions

$$dn/ds = \pm \tan\mu \quad (12)$$

where μ is the crossflow Mach angle defined in terms of the crossflow Mach number $M = q/a$ by

$$\sin\mu = 1/M \quad (13)$$

Along these curves disturbances are propagated on the unit sphere satisfying the compatibility condition obtained from Eqs. (4) and (7),

$$\frac{d\beta}{dn} \pm \frac{a^2}{q^2} \frac{\cotan\mu}{\gamma p} \frac{dp}{dn} = \pm \cotan\mu \cos\beta \cotan\theta - \left(\frac{u}{q} + \sin\beta \cotan\theta \right) \quad (14)$$

Equation (12) defines the domain of dependence and the range of influence on the unit sphere of any point within the hyperbolic region. If the domain of dependence and the range of influence of a point include a portion of a boundary between the hyperbolic and elliptic region, then a disturbance at the point, through its influence on the elliptic region, may affect its own domain of dependence. Such a point is said to be in a pseudo-elliptic region. The boundary separating a pseudo-elliptic region from a properly hyperbolic region consists of a characteristic curve which is denoted the limiting characteristic. A detailed investigation of some of the properties of pseudo-elliptic regions occurring on conical delta wings with attached shocks is given in Ref. 9.

III. Properties of the Sonic Line

For two-dimensional flows, the flow properties attain constant critical conditions along the sonic line. For conical

flows, the situation is quite different. With the help of Bernoulli's equation

$$\frac{a^2}{\gamma-1} + \frac{u^2}{2} + \frac{q^2}{2} = \text{const} \quad (15)$$

it follows that along the sonic line ($a^2 = q^2$),

$$\frac{dq}{d\ell} = - \left(\frac{\gamma-1}{\gamma+1} \right) \frac{u^*}{q^*} \frac{du}{d\ell} \quad (16)$$

where $d\ell$ is an infinitesimal element of length along the sonic line, as indicated in Fig. 1, and the superscript * indicates critical conditions. Assuming that the flow is irrotational (see Appendix),

$$\partial u / \partial n = 0 \quad (17)$$

and we may write

$$du/d\ell = q^* ds/d\ell \quad (18)$$

With reference to Fig. 1, this can also be written in the form

$$du/d\ell = q^* \cos\alpha \quad (19)$$

Therefore,

$$\frac{dq}{d\ell} = - \left(\frac{\gamma-1}{\gamma+1} \right) u^* \cos\alpha \quad (20)$$

Equation (20) was first presented by Ferri in Ref. 9 in a slightly different form. The equation indicates that along the sonic line the crossflow velocity increases in the direction which makes an obtuse angle with the vector q , as indicated in Fig. 2. It is a simple matter to obtain the behavior of all the other flow properties along the sonic line. For example, the change in the speed of sound, the radial component of Mach number, and the pressure are given, respectively, by

$$\frac{da}{d\ell} = - \left(\frac{\gamma-1}{\gamma+1} \right) u^* \cos\alpha \quad (21)$$

$$\frac{d(u/a)}{d\ell} = \left[1 + \frac{\gamma-1}{\gamma+1} \left(\frac{u^*}{a^*} \right)^2 \right] \cos\alpha \quad (22)$$

$$\frac{1}{p^*} \frac{dp}{d\ell} = \frac{-2\gamma}{\gamma+1} \left(\frac{u^*}{a^*} \right) \cos\alpha \quad (23)$$

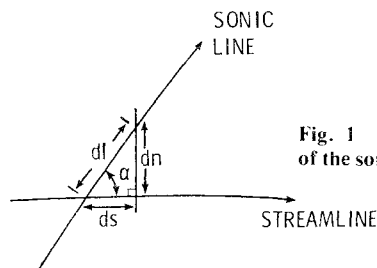


Fig. 1 Definition of the inclination of the sonic line to the streamline.

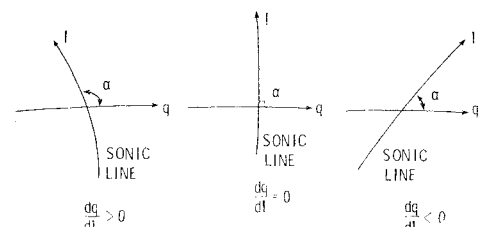


Fig. 2 Behavior of crossflow velocity along sonic line.

Other details of the flowfield in the neighborhood of the sonic line can be obtained by assuming that the velocity components are analytic functions of s and n . Then, with the help of Bernoulli's equation, Eq. (5), and assuming irrotational flow, we may write

$$q = a^* + q_n^* n + q_s^* s + \dots \quad (24a)$$

$$u = u^* + a^* s + \dots \quad (24b)$$

$$a = a^* - \frac{\gamma-1}{2} q_n^* n - \frac{\gamma-1}{2} (u^* + q_s^*) s + \dots \quad (24c)$$

$$\beta = \beta^* + (\cos\beta^* \cotan\theta^* + \frac{1}{a^*} q_n^*) s - \left(\frac{u^*}{a^*} + \sin\beta^* \cotan\theta^* \right) n + \dots \quad (24d)$$

$$p = p^* \left(1 - \gamma \left(\frac{u^*}{a^*} \right) \left(1 + \frac{1}{u^*} q_s^* \right) s - \frac{\gamma}{a^*} q_n^* n + \dots \right) \quad (24e)$$

Introducing the preceding Taylor expansions into the definition of the crossflow sonic line ($a^2 = q^2$), we obtain the sonic line slope

$$\frac{dn}{ds} \equiv \tan\alpha = - \left(\frac{\gamma-1}{\gamma+1} + \frac{1}{u^*} q_s^* \right) \frac{1}{u^*} q_n^* \quad (25)$$

Similarly, the slope of the isobar is given by

$$\frac{dn}{ds} \equiv \frac{-p_s^*}{p_n^*} = - \left(1 + \frac{1}{u^*} q_s^* \right) \frac{1}{u^*} q_n^* \quad (26)$$

and the slope of the line of constant crossflow velocity is given by

$$\frac{dn}{ds} = \frac{-q_s^*}{q_n^*} \quad (27)$$

Alternatively, these relations can be obtained directly from Eq. (5, 6, 11, and 15).

IV. Properties of Mach Lines at Sonic Line

The angle made by the Mach line and the normal to the meridional plane ϕ , at some point along the sonic line, is given by $\epsilon = \beta \pm \mu$. Following the lead of Ref. 5, a measure of the curvature of the Mach lines, $d\epsilon/dn$ can be obtained from the compatibility condition, Eq. (14). In the neighborhood of the sonic line, we have

$$\frac{d\epsilon}{dn} \approx \pm \frac{1}{a} \frac{\gamma+1}{2} \frac{1}{\cos\mu} \frac{dq}{dn} + O(1) \quad (28)$$

At a singular point of the sonic line, the sonic line is tangent to the Mach line and a weak singularity of the flow variables may occur across the sonic line. From Eq. (25), it follows that at such a point

$$\partial q / \partial n = 0 \quad (29)$$

and, since the sonic line is tangent to the Mach line, $dq/dn=0$, the curvature of the Mach line is finite. At non-singular sonic points the curvature is infinite.

Again following Ref. 5, the coordinates of either Mach line near a sonic point may be represented by a power series

$$n = \sum_{i=1}^{\infty} a_i \nu^i \quad (30a)$$

$$s = \sum_{i=1}^{\infty} b_i \nu^i \quad (30b)$$

where $\nu = (\pi/2) - \mu$. Since for a nonsingular sonic point, both the slope and curvature of each Mach line are infinite at the sonic point, we can anticipate that $b_1 = b_2 = 0$. The remaining coefficients in the series can be found by expanding the Mach line slope

$$\frac{ds}{d\nu} = \pm \cotan\nu \quad (31)$$

and the strip condition satisfied on a Mach line

$$\frac{dq}{d\nu} = q_n^* \frac{dn}{d\nu} + q_s^* \frac{ds}{d\nu} \quad (32)$$

and equating coefficients of equal powers. After some manipulation, the results are:

$$n = \frac{a^*}{\gamma+1} \frac{1}{q_n^*} \nu^2 \pm \frac{2}{3} \frac{a^*}{\gamma+1} \frac{1}{q_n^{*2}} \left(\frac{\gamma-1}{\gamma+1} u^* + q_s^* \right) \nu^3 + \dots \quad (33a)$$

$$s = \pm \frac{2}{3} \frac{a^*}{\gamma+1} \frac{1}{q_n^*} \nu^3 + \dots \quad (33b)$$

The leading terms are the same as the leading terms in two-dimensional flow (see Ref. 5), but the higher-order terms are different. As in the two-dimensional flow, near a sonic point each Mach line behaves like a branch of the semicubical parabola

$$n^3 = \frac{9}{4} \frac{a^*}{\gamma+1} \frac{1}{q_n^*} s^2 \quad (34)$$

with a cusp at the sonic point. At a singular sonic point ($q_n^* = 0$), the curvature of the Mach line is finite and we must retain the coefficient b_2 . Proceeding as before, the leading terms of the series are:

$$n = \frac{\pm 2a^*}{(\gamma-1)u^* + (\gamma+1)q_s^*} \nu + \dots \quad (35a)$$

$$s = \frac{a^*}{(\gamma-1)u^* + (\gamma+1)q_s^*} \nu^2 + \dots \quad (35b)$$

Therefore, near a singular sonic point, each Mach line behaves like a branch of the parabola

$$n^2 = \frac{4a^*}{(\gamma-1)u^* + (\gamma+1)q_s^*} s \quad (36)$$

which, unlike the two-dimensional results, defines only two real Mach lines at the sonic point.

V. Jump Conditions at a Singular Sonic Point

As discussed before, when the sonic line is normal to the streamline and, therefore, tangent to the Mach line, a weak singularity occurs across the sonic line. In the linearized theory of conical flows, the pressure downstream of the sonic line behaves like $p \sim \pm \sqrt{s}$ so that the pressure gradient goes to $\pm \infty$ at the sonic line ($s=0$). In Ref. 10, Lighthill shows that

the linear theory is the first term in a series which diverges near the sonic line and that the true behavior of the pressure gradient is:

$$\left. \frac{1}{p^*} \frac{\partial p}{\partial s} \right|_* \sim \frac{2\gamma}{\gamma+1} \frac{M_\infty^2 - 1}{M_\infty^2}$$

if the pressure increases downstream of the sonic line, in which case the sonic line may be replaced by a crossflow shock wave, and

$$\left. \frac{1}{p^*} \frac{\partial p}{\partial s} \right|_* \sim -\frac{\gamma}{\gamma+1} \frac{M_\infty^2 - 1}{M_\infty^2}$$

if the pressure decreases downstream of the sonic line, where M_∞ is the freestream Mach number. The sonic line remains, however, singular, since some of the first derivatives of the flow variables are discontinuous at the sonic line.

The constraints on the jumps of the first derivatives may be obtained from Eqs. (4-8). Denoting the jump of the first derivative of a flow variable across the sonic line by

$$[f] = f_1 - f_2 \quad (37)$$

where the subscripts 1 and 2 indicate upstream and downstream values, respectively, we have

$$[S_n] = [S_s] = [u_n] = [u_s] = [\beta_n] = [\beta_s] = [p_n] = [q_n] = 0 \quad (38)$$

and

$$[q_s] = \frac{-a^*}{\gamma p^*} [p_s] = \frac{-2}{\gamma - 1} [a_s] \quad (39)$$

The behavior of the flowfield near a singular sonic point may be investigated further by writing Eq. (6) with the help of Eq. (5) in the form

$$u_{ss} + u = (-a^2/\gamma qp) p_s \quad (40)$$

If we assume that near the sonic point the right-hand side of Eq. (40) behaves like some delta function $h(s)$, such that

$$h(s) = \begin{cases} h_+, & s > 0 \\ h_-, & s < 0 \end{cases} \quad (41)$$

and u satisfies the boundary conditions

$$u(0) = u^* \quad (42a)$$

$$u_s(0) = a^* \quad (42b)$$

then the following results are obtained

$$\frac{u}{u^*} = \left(1 - \frac{h}{u^*}\right) \cos(s) + \frac{a^*}{u^*} \sin(s) + \frac{h}{u^*} \quad (43a)$$

$$\frac{q}{u^*} = -\left(1 - \frac{h}{u^*}\right) \sin(s) + \frac{a^*}{u^*} \cos(s) \quad (43b)$$

$$\begin{aligned} \frac{a^2}{u^{*2}} = & \left(\frac{a^*}{u^*}\right)^2 + (\gamma - 1) \frac{h}{u^*} \left[\left(1 - \frac{h}{u^*}\right) \right. \\ & \times (1 - \cos(s)) - \frac{a^*}{u^*} \sin(s) \left. \right] \end{aligned} \quad (43c)$$

The value of h for $s > 0$ depends, because of the transonic nature of the problem, on the global solution and cannot be predicted in general by the present local analysis. However,

for the case of a delta wing with diamond cross section, Roe¹¹ has obtained the exact values for the gradients on the downstream side of the sonic line. They are:

$$\frac{1}{u^*} q_s^* = \frac{-\gamma}{\gamma + 1} \quad (44a)$$

$$\frac{1}{p^*} p_s^* = \frac{-\gamma}{\gamma + 1} \left(\frac{u^*}{a^*}\right) \quad (44b)$$

and, therefore, for this case

$$h_+ = \frac{u^*}{\gamma + 1} \quad (45)$$

VI. Flow Patterns at a Sonic Point

An overall picture of the possible flow patterns at a crossflow sonic point can be constructed by introducing the Taylor series expansion given by Eq. (24) into Eq. (10) and equating like powers. The resulting expressions are then a function of $\partial g/\partial s|_*$ and $\partial g/\partial n|_*$, where

$$g = \beta_n + \sin\beta \cot\alpha \quad (46)$$

A more significant result can be obtained by evaluating $\partial g/\partial s|_*$ and $\partial g/\partial n|_*$ through differentiation of Eq. (10). Performing this operation, the resulting expressions are:

$$\frac{1}{u^*} q_s^* = \frac{-\gamma}{\gamma + 1} \left[1 \pm \sqrt{1 - 2 \frac{(\gamma + 1)}{\gamma^2} \left(\xi + \frac{\gamma - 1}{2} \right)} \right] \quad (47)$$

$$\frac{1}{u^*} q_n^* = \xi / \left(\frac{\gamma + 1}{2} \right) \left(1 + \frac{1}{u^*} q_s^* \right) \tan\alpha \quad (48)$$

where

$$\xi = \frac{1}{p^*} \left(\frac{a^*}{u^*} \right) \frac{\partial p}{\partial s} \bigg|_* \frac{\partial M}{\partial s} \bigg|_* \quad (49)$$

The behavior of q_s^* as a function of ξ is shown in Fig. 3 for an adiabatic exponent of 7/5. Different regions may be defined in Fig. 3 by considering the rate of change of the crossflow Mach number along a crossflow streamline given with the help of Bernoulli's equation and Eq. (5) by

$$\frac{\partial M}{\partial s} \bigg|_* = \frac{1}{2} \frac{u^*}{a^*} \left((\gamma + 1) \frac{1}{u^*} q_s^* + (\gamma - 1) \right) \quad (50)$$

A streamline crossing the sonic line transitions from an elliptic region to a hyperbolic region, and vice versa, across

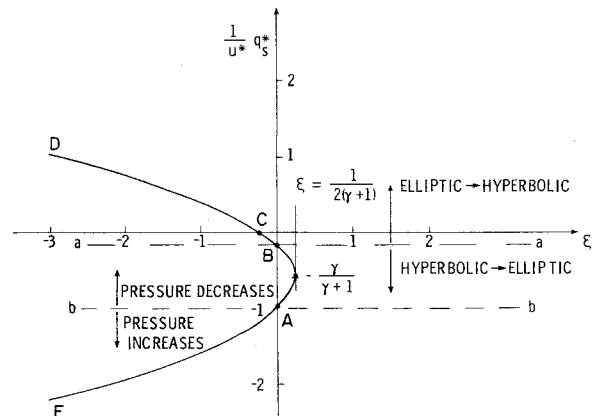


Fig. 3 Different flow regimes at a crossflow sonic point.

Fig. 4 Sketch of a cone at angle of attack with supersonic cross-flow bubble.

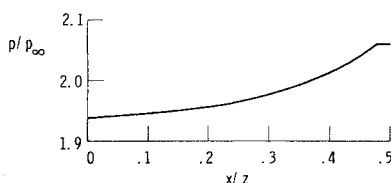
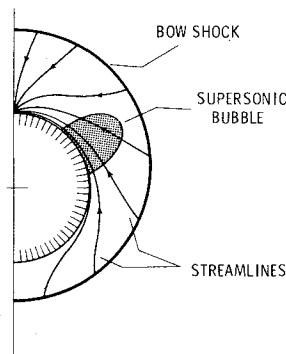


Fig. 5 Computed surface pressure distribution over a delta wing with swept back leading edges.

the line

$$\frac{1}{u^*} q_s^* = -\left(\frac{\gamma-1}{\gamma+1}\right) \quad (51)$$

This dividing line is labeled *aa* in Fig. 4. Also, from Eq. (6) it follows that the line

$$(1/u^*)q_s^* = -1 \quad (52)$$

separates a region where the pressure increases along a streamline from a region where it decreases. This dividing line is labeled *bb* in Fig. 3.

It is apparent from Fig. 3 that a streamline crossing a crossflow sonic line from an elliptic to a hyperbolic region is always accompanied by a decrease in pressure. This is the case, for example, for streamlines entering the supersonic crossflow bubble that forms on cones at high angles of attack, as sketched in Fig. 4. However, a streamline crossing a crossflow sonic line from a hyperbolic region to an elliptic region can be accompanied by either a pressure increase or a pressure decrease. This behavior is unlike two-dimensional flow where the pressure always increases as a streamline crosses from a hyperbolic to an elliptic region.

As an example, consider the flow over a delta wing with a compression angle of 10 deg and leading edges swept back 20 deg flying at Mach 3 as shown on Fig. 5. The computed¹² value for $(1/u^*)q_s^*$ at the surface of the wing is -0.761 . This value is somewhat off from the exact value of -0.583 predicted by Roe.¹¹ Three reasons account for this error: 1) the first derivative q_s^* is computed to first-order accuracy only; 2) the gradients at the sonic line are large and, therefore, the truncation error is large; and 3) the grid used in Ref. 12 was rather coarse in the neighborhood of the sonic line.

If the wing leading edges are swept forward 20 deg, as indicated in Fig. 6, the pressure then increases inside the Mach cone, as shown in Fig. 6, with a computed¹² value for $(1/u^*)q_s^*$ of -2.12 consistent with the results of Fig. 3. For this case, the sonic line should be replaced by a crossflow shock, and the analysis of Roe¹¹ is no longer valid. The

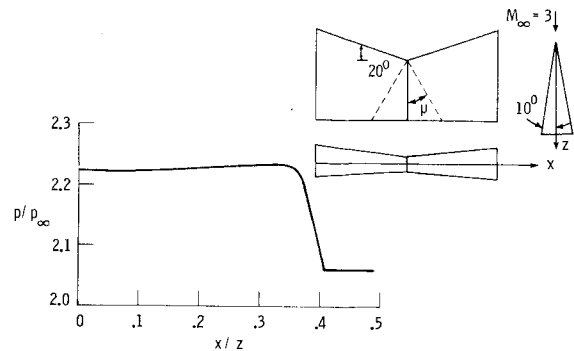


Fig. 6 Computed surface pressure distribution over a delta wing with swept forward leading edges.

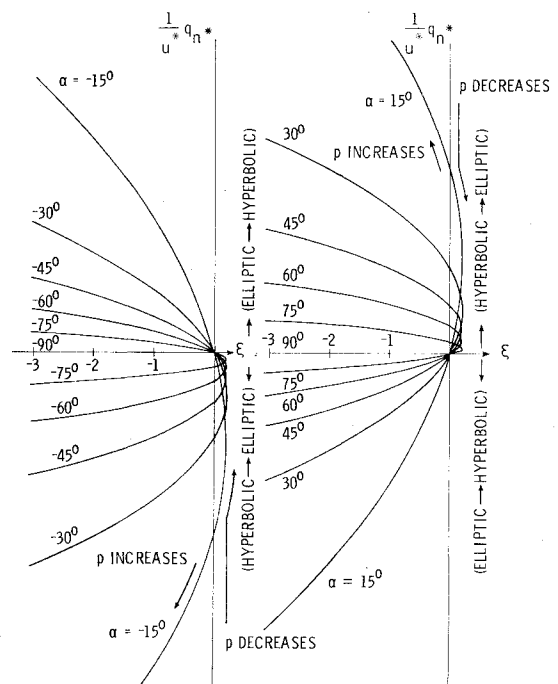


Fig. 7 Behavior of q_n^* at a crossflow sonic point.

computed¹² crossflow shock for this case was captured and the results are only qualitatively good.

The behavior of q_n^* as a function of ξ is shown on Fig. 7 for both negative (Fig. 7a) and positive (Fig. 7b) inclinations of the sonic line to the streamline. The different regions are shown in the figure. For each curve representing a constant negative inclination, the pressure along a crossflow streamline decreases in the fourth quadrant as indicated for $\alpha = -15$ deg. For positive inclinations, the pressure decreases in the first quadrant, as indicated in the figure. When the sonic line becomes tangent to the streamline ($\alpha = 0$), q_n^* becomes indeterminate.

On Fig. 3, point A corresponds to a streamline crossing a crossflow sonic line with zero pressure gradient on the hyperbolic side. From Eq. (48), it is seen that the value of q_n^* is undetermined since both numerator and denominator vanish at A. An important case, since it occurs on delta wings with uniform flow in the hyperbolic region,⁹ corresponds to zero q_n^* ($\alpha = 90$ deg). Point A is then a singular sonic point with the Mach lines tangent to the sonic line. (This was the case for the two delta wings shown on Figs. 5 and 6.) In that case, the value of q_s^* in the downstream side of the sonic line is governed by the jump conditions given by Eq. (39). Depending, in general, on the global solution to the problem, the downstream value of q_s^* can be somewhere along the arc EA

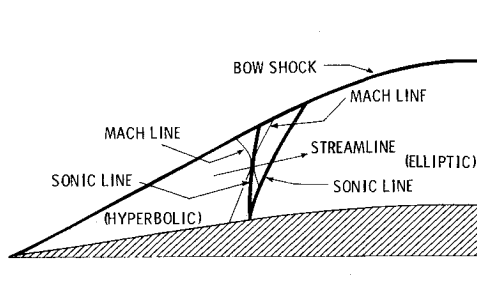


Fig. 8 Double sonic line on a delta wing as described by Ferri.

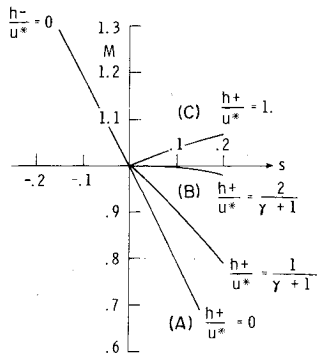


Fig. 9 Crossflow Mach number behavior near a singular sonic point for different values of h_+/u^* . Correspondence to points on Fig. 3 in parentheses.

on Fig. 3 if the pressure gradient increases, or along the arc DA if the pressure gradient decreases.

In Ref. 13, it was proven that q_s^* is bounded in the range $\xi \geq 0$ and from this it was concluded that q_s^* is nonsingular. It is clear from Fig. 3 that q_s^* is bounded for all finite values of ξ . However, this does not preclude q_s^* from being weakly singular, since it can be multivalued, as just described.

At such a singular sonic point, if the magnitude of the pressure gradient is sufficiently large, such that the downstream side of the sonic line corresponds to some point along the arc BD of Fig. 3, then a situation similar to that occurring on a Laval nozzle with supersonic flow on both sides of a throat occurs. The possibility of a second sonic line, as sketched on Fig. 8, was speculated by Ferri in Ref. 9, and, as will be shown, was incorrectly refuted by Reyn in Ref. 8.

The behavior of the flow near the sonic line under the previously described conditions can be predicted using the results of Sec. V. For example, upstream of the sonic line, at point A on Fig. 3 corresponding to $h_- = 0$, the crossflow Mach number behaves like

$$M = \cos(s) - (u^*/a^*)\sin(s) \quad s < 0 \quad (53)$$

and downstream of the sonic line, corresponding to a jump on q_s^* somewhere along the arc AD on Fig. 3, the behavior is like

$$M = \left(\cos(s) - \frac{u^*}{a^*} \left(1 - \frac{h_+}{u^*} \right) \sin(s) \right) / \left(1 + (\gamma - 1) \left(\frac{h_+}{u^*} \right) \left(\frac{u^*}{a^*} \right) \right) \times \left[\left(1 - \frac{h_+}{u^*} \right) \left(\frac{u^*}{a^*} \right) (1 - \cos(s)) - \sin(s) \right]^{1/2} \quad s > 0 \quad (54)$$

These results are plotted on Fig. 9 for $u^*/a^* = 2$ and several values of h_+/u^* . As can be seen from the figure, once the value of h_+/u^* exceeds $2/(\gamma + 1)$, the crossflow Mach number downstream of the sonic line becomes supersonic once again as predicted by Ferri.

This double crossflow sonic line feature has been found numerically¹² on a delta wing configuration which is truncated at the Mach cone as shown in Fig. 10. The crossflow Mach number on the surface of the wing plotted on Fig. 10

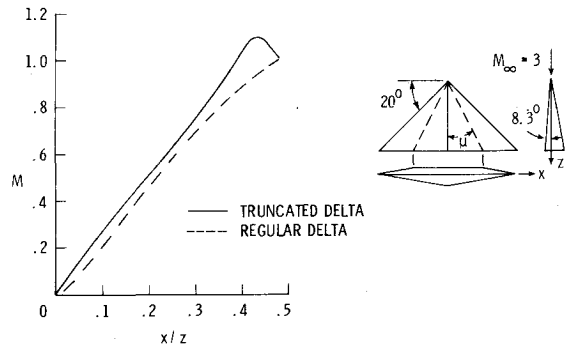


Fig. 10 Computed surface crossflow Mach number on a truncated and a regular delta wing.

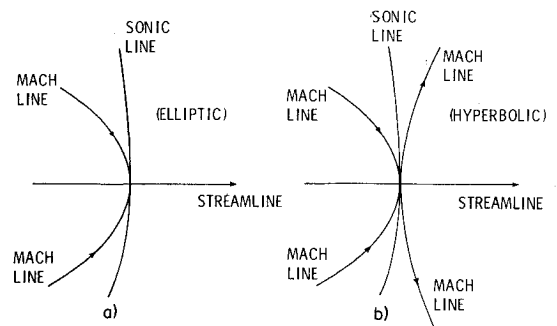


Fig. 11 Flow pattern at a singular sonic point. Isobars and constant crossflow lines coincide with sonic line.

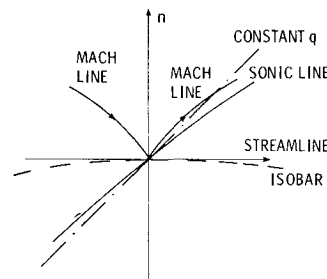


Fig. 12 Flow pattern at a regular sonic point, point A on Fig. 3.

shows the appearance of a second sonic line. The computed value of $(1/u^*) q_s^*$ is 0.056 in agreement with the requirements of Fig. 3.

The Mach line pattern at a singular sonic point, corresponding to point A of Fig. 3, is shown in Fig. 11a for the case where the downstream side is elliptic and in Fig. 11b for the case where it is hyperbolic. The flow pattern at a regular sonic point A is shown in Fig. 12. The flow pattern occurring when the sonic line is tangent to the streamline, corresponding to point B on Fig. 3, is shown in Fig. 13.

VII. Observations About Supersonic Crossflow Bubbles

When a subsonic crossflow is sufficiently accelerated, a bubble of locally supersonic crossflow partially bounded by the body contour is formed as shown, for example, in Fig. 4. This is also a common situation in two-dimensional flows over airfoils with freestream Mach numbers above a certain critical Mach number. For two-dimensional flows, many of the properties of these supersonic bubbles are well known.¹⁴ Perhaps one of the most important properties of these bubbles is the Nikolskii-Taganov rule for the monotonic decrease of the streamline slope along the sonic line as an observer moves along the sonic line in the direction of the flow.¹⁴ The determination of these flow properties for two-dimensional flows has been greatly helped by the fact that the flow attains

Fig. 13 Flow pattern at a regular sonic point, point B on Fig. 3.

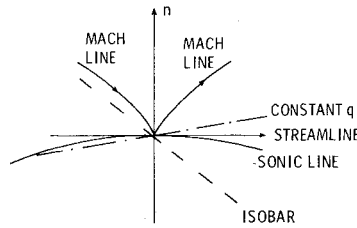
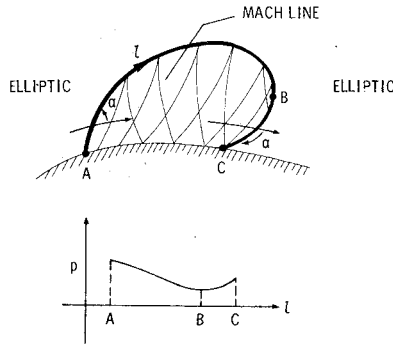


Fig. 14 Hypothetical supersonic crossflow bubble and corresponding pressure distribution along sonic line.



constant critical conditions along the sonic line and that along a characteristic, the magnitude of the velocity is only a function of the streamline inclination. For conical flows the situation is more complex. Because of these complexities, we will only make some qualitative observations here about the structure of these bubbles.

Recent numerical calculations of flows over elliptical and circular cones^{15,16} indicate that the inclination of the sonic line to the streamline α decreases monotonically along the sonic line as an observer moves along the sonic line in the direction of the flow. If this is the case, then it follows from Eq. (23) that the pressure along the sonic line will continuously decrease until the sonic line makes an obtuse angle with the streamline, as indicated in the sketch of Fig. 14. The numerical results,^{15,16} however, indicate that the shape of the sonic line is such that where it meets the body contour its inclination is not greater than a right angle. Indeed, for a circular cone, with cone half-angle θ_c , it can be shown, with Eqs. (7) and (11), that

$$q_n/u = (-q/u) \cot \alpha \quad (55)$$

on the cone surface, and since it follows from Fig. 3 that at the point where the streamline on the surface of the cone exits from the supersonic bubble

$$\frac{\gamma-1}{\gamma+1} + \frac{1}{u^*} q_s^* \leq 0 \quad (56)$$

we must conclude that

$$\tan \alpha \leq 0 \quad (57)$$

Therefore, for a circular cone at the point on the cone surface where the streamline exits the bubble, the inclination of the sonic line must be less than a right angle. The pressure on the surface of the body must then decrease from its value at the point where the streamline enters the bubble to the value where it exits the bubble. However, if the pressure is reduced within the supersonic region to a value lower than its value downstream of the bubble (as apparently must be the case if the bubble is relatively close to the symmetry plane, since the pressure downstream of the bubble is the high pressure associated with a stagnating crossflow), then the supersonic bubble must terminate with a crossflow shock in order to match the downstream pressure level. Thus, the prevention of crossflow shock waves for these conical transonic flows

appears considerably more difficult than it already is for two-dimensional flows.

The preceding observations are made because of their importance in the design of shock-free conical or quasiconical wings.¹⁷ These observations, however, lack the rigor of the previous sections of this paper and must, of course, be used intelligently.

Appendix

The rate of change of entropy on the surface of the unit sphere is given by¹⁸:

$$\frac{1}{\gamma} \frac{a^2}{\gamma-1} \frac{\partial S}{\partial \theta} = -u \frac{\partial u}{\partial \theta} - w \frac{\partial w}{\partial \theta} + \frac{w}{\sin \theta} \frac{\partial v}{\partial \phi} + uv - w^2 \cot \theta \quad (A1)$$

$$\begin{aligned} \frac{1}{\gamma} \frac{a^2}{\gamma-1} \frac{1}{\sin \theta} \frac{\partial S}{\partial \phi} &= v \frac{\partial w}{\partial \theta} - \frac{u}{\sin \theta} \frac{\partial u}{\partial \phi} \\ &- \frac{v}{\sin \theta} \frac{\partial v}{\partial \phi} + uw + vw \cot \theta \end{aligned} \quad (A2)$$

introducing q and β we may write,

$$\begin{aligned} \frac{1}{\gamma} \frac{a^2}{\gamma-1} \frac{\partial S}{\partial \phi} &= -u \frac{\partial u}{\partial \theta} + q \left(u \sin \beta - \left(\frac{\partial q}{\partial n} \right. \right. \\ &\left. \left. - q \frac{\partial \beta}{\partial s} \right) \cos \beta - q \cos \beta^2 \cot \theta \right) \end{aligned} \quad (A3)$$

$$\begin{aligned} \frac{1}{\gamma} \frac{a^2}{\gamma-1} \frac{1}{\sin \theta} \frac{\partial S}{\partial \phi} &= -\frac{u}{\sin \theta} \frac{\partial u}{\partial \phi} + q \left(u \cos \beta \right. \\ &\left. + \left(\frac{\partial q}{\partial n} - \frac{\partial \beta}{\partial s} \right) \sin \beta - q \sin \beta \cos \beta \cot \theta \right) \end{aligned} \quad (A4)$$

These two equations may be expressed in the form

$$\frac{1}{\gamma} \frac{a^2}{\gamma-1} \frac{\partial S}{\partial s} = u \left(q - \frac{\partial u}{\partial s} \right) \quad (A5)$$

$$\frac{1}{\gamma} \frac{a^2}{\gamma-1} \frac{\partial S}{\partial n} = -u \frac{\partial u}{\partial n} - q \left(\frac{\partial q}{\partial n} - q \frac{\partial \beta}{\partial s} + q \cos \beta \cot \theta \right) \quad (A6)$$

Using Eq. (5), Eq. (A5) results in

$$\partial S / \partial s = 0 \quad (A7)$$

and, since the radial component of vorticity ($\Omega = \nabla \times \mathbf{V}$) on the surface of the unit sphere is given by

$$\Omega_r = \frac{\partial q}{\partial n} - q \frac{\partial \beta}{\partial s} + q \cos \beta \cot \theta \quad (A8)$$

we may conclude that if the flow is irrotational

$$u \frac{\partial u}{\partial n} = 0 \quad (A9)$$

Acknowledgment

The author is grateful to D. Anderson of Iowa State University for his review of this paper, J. Daywitt of General Electric for bringing to the author's attention the work of P. L. Roe, and G. DaForno of Grumman Aerospace Corporation for many helpful discussions.

References

- ¹Legendre, R., "Vortex Sheets Rolling-Up Along Leading Edges of Delta Wings," *Progress in Aeronautical Sciences*, Vol. 7, edited by D. Küchemann, et al., Pergamon Press, New York, 1966, pp. 7-33.
- ²Werle, H., "Essai de Vérification de la Conicité de l'Écoulement Autour d'une Aile delta Mince avec Incidence," R.A. No. 63, 1958.
- ³Busemann, A., "Drücke Auf Kegelförmige Spitzen bei Bewegung mit Überschallgeschwindigkeit," *Zeitschrift für Angewandte Mathematik und Mechanik*, Vol. 9, 1929, pp. 496-498.
- ⁴Lighthill, M. J., "The Hodograph Transformation in Trans-sonic Flow, I. Symmetric Channels," *Proceedings of the Royal Society, Series A*, 191, 1947, p. 323.
- ⁵Holt, M., "Flow Patterns and the Method of Characteristics Near a Sonic Line," *Quarterly Journal of Mechanical and Applied Mathematics*, Vol. II, Pt. 2, 1949, pp. 246-256.
- ⁶Landau, L. D. and Lifshitz, E. M., *Fluid Mechanics*, Pergamon Press, London, 1959, pp. 436-456.
- ⁷Ferrari, C. and Tricomi, F. G., *Transonic Aerodynamics*, Academic Press, New York, 1968.
- ⁸Reyn, J. W., "Differential-Geometric Considerations on the Hodograph Transformation for Irrotational Conical Flows," *Archive for Rational Mechanics and Analysis*, Vol. 6, No. 4, 1960, pp. 299-354.
- ⁹Ferri, A., Vaglio-Laurin, R., and Ness, N., "Mixed Type Conical Flow without Axial Symmetry," Polytechnic Institute of Brooklyn, PIBAL Rept. No. 264, 1954.
- ¹⁰Lighthill, M. J., "The Shock Strength in Supersonic Conical Fields," *Philosophical Magazine*, Ser. 7, Vol. 40, 1949, pp. 1202-1223.
- ¹¹Roe, P. L., "A Result Concerning the Supersonic Flow Below a Plane Delta Wing," Aeronautical Research Council, CP. No. 1228, April 1972.
- ¹²Salas, M. D., "A Careful Numerical Study of Flow Fields About External Conical Corners: Part I, Symmetric Configurations," AIAA Paper 79-1511, July 1979.
- ¹³Scheuing, R. A. Hayes, W. D., et al., "Theoretical Prediction of Pressures in Hypersonic Flow with Special Reference to Configurations Having Attached Leading-Edge Shocks. Part I. Theoretical Investigation," Wright-Patterson Air Force Base, Ohio, ASD-TR 61-60, 1962.
- ¹⁴Nikolskii, A. A. and Taganov, G. I., "Gas Motion in a Local Supersonic Region and Conditions of Potential-Flow Breakdown," NACA, TM No. 1213, May 1949.
- ¹⁵Grossman, B., "A Numerical Procedure for the Computation of Supersonic Conical Flows," AIAA Paper No. 78-1213, July 1978.
- ¹⁶Siclari, M. J., "Investigation of Crossflow Shocks on Delta Wings in Supersonic Flows," AIAA Paper 79-0345, Jan. 1979.
- ¹⁷Mason, W. H. and DaForno, G., "Opportunities for Supersonic Performance Gains Through Non-Linear Aerodynamics," AIAA Paper 79-1527, July 1979.
- ¹⁸Ferri, A., "Supersonic Flows with Shock Waves," Sec. H. of *General Theory of High-Speed Aerodynamics*, Vol VI of *High-Speed Aerodynamics and Jet Propulsion*, Princeton University Press, Princeton, N.J., 1954, pp. 721-726.

From the AIAA Progress in Astronautics and Aeronautics Series..

EXPERIMENTAL DIAGNOSTICS IN COMBUSTION OF SOLIDS—v. 63

Edited by Thomas L. Boggs, Naval Weapons Center, and Ben T. Zinn, Georgia Institute of Technology

The present volume was prepared as a sequel to Volume 53, *Experimental Diagnostics in Gas Phase Combustion Systems*, published in 1977. Its objective is similar to that of the gas phase combustion volume, namely, to assemble in one place a set of advanced expository treatments of the newest diagnostic methods that have emerged in recent years in experimental combustion research in heterogenous systems and to analyze both the potentials and the shortcomings in ways that would suggest directions for future development. The emphasis in the first volume was on homogenous gas phase systems, usually the subject of idealized laboratory researches; the emphasis in the present volume is on heterogenous two- or more-phase systems typical of those encountered in practical combustors.

As remarked in the 1977 volume, the particular diagnostic methods selected for presentation were largely undeveloped a decade ago. However, these more powerful methods now make possible a deeper and much more detailed understanding of the complex processes in combustion than we had thought feasible at that time.

Like the previous one, this volume was planned as a means to disseminate the techniques hitherto known only to specialists to the much broader community of reeseach scientists and development engineers in the combustion field. We believe that the articles and the selected references to the current literature contained in the articles will prove useful and stimulating.

339 pp., 6 × 9 illus., including one four-color plate, \$20.00 Mem., \$35.00 List

TO ORDER WRITE: Publications Dept., AIAA, 1290 Avenue of the Americas, New York, N.Y. 10019